Journal of Solid State Chemistry **147,** 379–389 (1999)
Article ID jssc.1999.8381, available online at http://www.idealibrary.com on IDEAL®

Structure and Bonding Anisotropy in Intergrowth Oxides: A Clue to the Manifestation of Bidimensionality in *T*-, *T*′-, and *T**-Type Structures

J. Choisnet

CRMD-Cristallochimie, Université d'Orléans, 45067 Orléans Cedex 2, France

Received October 26, 1998; in revised form May 4, 1999; accepted May 21, 1999

The manifestation of bidimensionality in *T*-, *T*′-, and *T-type structures of A_2BO_4 oxides occurs in terms of cooperative structure–bonding properties involving both the metal–oxygen *A*(*B*)–O bonds and the *A*–*A* cationic repulsions. The analysis of the *A*-metal network gives evidence of ninefold cationic coordination very similar to the ninefold oxygen coordination. The short *A*–*A* apical distance results in *A*–*A* repulsions which are able to balance the *A*–O apical overbonding. In La_2NiO_4 as compared to La_2CuO_4, the contribution of these repulsions is more important (d_{A-A} = 3.25 Å in La_2NiO_4; 3.66 Å in La_2CuO_4). The perovskite (P)/rock salt (RS) intergrowth, *T*-type structure, due to strong geometrical constraint, has excess anisotropy which needs to be relieved. In contrast, the perovskite (P)/calcium fluoride (CF), *T*′- type structure, is nearly free from any excess anisotropy to be relieved. In the (P)/(RS)/(P)/(CF) intergrowth, *T**-type structure, owing to a more regular distribution of the *A*–O bonds, the excess anisotropy is further restricted. Crystal chemical mechanisms such as *A* substitutions and the oxidation of Cu, which lower the excess charge in the anionic and cationic (P) and (RS) slabs, respectively, do not operate. The useful role of controlled excess structure–bonding anisotropy is emphasized.** © 1999 Academic Press

INTRODUCTION

Low-dimensional (LD) solids have a major contribution to the development of solid state chemistry in the last decades. The typical properties which are related to the low dimensionality are among the most interesting known in solids. As Jean Rouxel emphasized (1), "the greatest conceptual richness of (LD) solids is likely to be found in their outstanding chemical reactivity." With regard to this, the intercalation reactions and even more, the deintercalation reactions regarded as "a reciprocal chemistry of the intercalation" (1) usually are worked out under the conditions of the so-called "chimie douce": they are the route to a number of syntheses of new solids or at least new forms of known solids which cannot be prepared using the classical high-temperature solid-state reactions. Certainly, the best examples of this chemistry are represented by nonoxide ionocovalent materials such as the *A*-intercalated layered mixed chalcogenides $A_xM_yX_z$ (X = S, Se, Te; $M = d$ transition metal) (2).

Compared to chalcogenides, oxides which are more electronegative do not show as much ability for anion–cation redox competition and consequently are not a concern of this new solid state chemistry, whose theoretical modeling of the chemical bonding is asymmetrical with regard to the bonding by electrons, i.e., is based on the creation of holes in antibonding levels (3). Nevertheless, oxides present repeated examples of (LD) solids, mainly layered ones, and furthermore, they are excellent candidates to trigger a progressive weakening of the dimensionality. This results in the formation of intermediate systems in terms of structure and bonding, which are interesting regarding both their physical properties and their chemical reactivity.

Of particular interest is the occurrence of bidimensionality (2D) in purely three-dimensional (3D) oxide materials. Depending on the development of anisotropy of the chemical bonding, the occurrence of the 2D has to be estimated, to a large extent, in terms of crystal chemical mechanisms which involve basically the connection of the geometrical and the bonding characteristics. In this respect, the investigation of the structure and bonding anisotropy in intergrowth oxides is likely to be the most informative step in the understanding of the manifestation of bidimensionality in oxide materials.

In the following, we report on an analysis of structure and bonding anisotropy in A_2BO_4 oxides such as nickelates, cuprates, and aluminates, whose structure is the 1/1 intergrowth of perovskite (P) and rock salt (RS) or fluorite (CF) slabs, i.e., the K_2NiF_4 *T*-type and Nd_2CuO_4 *T*′-type structure, respectively. From this, we focus on the peculiarity of the bidimensionality in the case of the double intergrowth of the *T**-type structure, as characterized in the new cuprates $Nd_{1.2}Sr_{0.8-x}Y(Ln)_xCuO_{4-\delta}$ (Ln = Ho, Er, Yb) (4). In the occurrence of the bidimensionality in the A_2BO_4 oxides, we

0022-4596/99 $30.00

emphasize the major contribution of the cooperative structure and bonding anisotropy of the *B* and *A* elements in the (P) and (RS) or (CF) slabs, respectively.

STRUCTURE-BONDING ANISOTROPY IN THE *T* AND *T′* TYPE STRUCTURES

The (P)/(RS) Intergrowth of the T-Type A_2BO_4 Oxides

The existence of the (P) $\equiv ABO_3$/(RS) $\equiv AO$ 1/1 intergrowth of the A_2BO_4 oxides is related to the working of a well-known geometrical property: the "*A*O" plane is a common plane of the (P) and (RS) slabs (Fig. 1a), i.e., perfect matching between the two slabs requires, as deduced from the connection of the (BO_6) octahedron with the ninefold oxygen coordination polyhedra of *A* (Fig. 1b), the following mathematical expression to be verified:

$$d_{A\text{-O}(2)}/d_{B\text{-O}(1)} = \sqrt{2}$$

The ionic model of chemical bonding, always considered in calculating the metal–oxygen distances in oxides, gives a good representation of the constraint resulting from this geometrical condition. In the *T*-type oxides, the value of the ratio $d_{A\text{-O}(2)}/d_{B\text{-O}(1)}$ modeled from the ionic radii (5) is significantly smaller than $\sqrt{2}$; for example, its value is close to 1.21 in La_2CuO_4, 1.25 in La_2NiO_4, and 1.31 in the aluminates $LaAAlO_4$ (A = Ca, Sr). From the structural data, the experimental value of this ratio is found to be rather close to $\sqrt{2}$, namely 1.45 in La_2CuO_4 (6), 1.43 in La_2NiO_4 (7), and 1.42 in $LaSrAlO_4$ (8). Very informative is the systematic trend which leads to this result, i.e., a simultaneous shortening of the equatorial $d_{B\text{-O}(1)}$ distances and lengthening of the in-plane $d_{A\text{-O}(2)}$ distances. Consequently, solving the geometrical problem set by the existence of the intergrowth is understood in terms of a strong anisotropy of the chemical bonding:

— There is an "overbonding" in the (BO_2) equatorial planes which is coupled to an "underbonding" in the (*A*O) one.

If one takes into account the breakdown of the valence-sum rule which occurs in such a case (9), this excess anisotropy has to be relieved to ensure the formation of the (P)/(RS) intergrowth. Two main geometrical mechanisms make a significant contribution to this relaxation; their precise occurrence is variable, depending on the kind of A_2BO_4 oxides:

— The shift of the apical oxygen toward the *A* metal (Fig. 1b) triggers a lengthening of the apical $d_{B\text{-O}(2)}$ distance coupled with a shortening of the apical $d_{A\text{-O}(2)}$ distance. As a result, there is a further extension of the cooperative underbonding–overbonding effects which develop on a continuous path from the (BO_2) equatorial planes to the (*A*O) one. In the cuprates, nickelates, and aluminates, the shift of the apical oxygen is always observed, but it decreases progressively from La_2CuO_4, where it is largest (elongation close to 27%) due to the supplementary contribution of the electronic Jahn–Teller effect, to La_2NiO_4 (16%) and even more to aluminates (9%).

— The buckling distortions of the (BO_2) equatorial plane (10, 11) are of importance both for La_2CuO_4 and for La_2NiO_4: they allow some relief of the overbonding in the (CuO_2) equatorial planes. They exist in air-prepared La_2CuO_4 and only in vacuum-prepared La_2NiO_4, as they

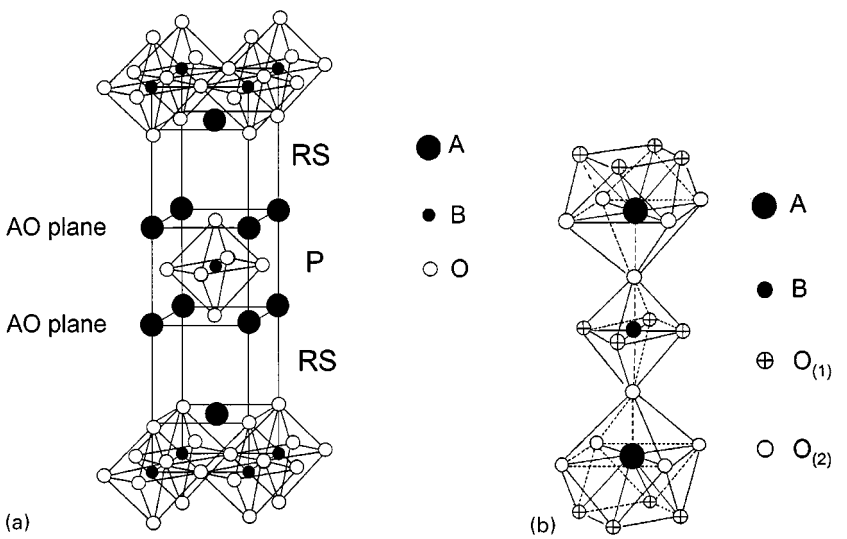

FIG. 1. (a) (P)/(RS) intergrowth of the *T*-type A_2BO_4 oxides (b) Connection of the (BO_6) octahedron and the ninefold oxygen coordination polyhedra of *A*.

are absent when the nickelate is air-prepared. Once more, the distortion is more significant in the cuprate than in the nickelate and it is unknown in the aluminates, because the relief of the constraint is achieved by the shift of the apical oxygen toward the A metal.

The structure–bonding properties of the ninefold coordination polyhedra of the A metal make their own contribution to the overall anisotropy of the T-type structure. This is analyzed further in a common description of the structure–bonding properties of the A metal in the T-, T'-, and T^*- type structures.

In the oxides where the excess anisotropy is large, namely cuprates and nickelates, the best relief is obtained by means of chemical mechanisms. These chemical mechanisms are rather numerous and at first sight seem to differ from each other. Considering a purely ionic model is enough to state the simple relationship which connects chemical reactivity and chemical bonding:

— The chemical mechanisms aim to "solve" the excess positive charge of the $(A_2O_2)^{u+}$ (RS) slabs and the excess negative charge of the $(BO_2)^{u-}$ equatorial planes.

The best examples are found in the crystal chemistry of La_2CuO_4 and La_2NiO_4, in agreement with the largest excess charge of the components of their intergrowth, $(La_2O_2)^{2+}$ and $(BO_2)^{2-}$. Under these conditions, one can separate two groups of mechanisms corresponding to

(i) a decrease of the excess positive charge of the $(La_2O_2)^{2+}$ slabs:

— heterovalent substitutions of A^{2+} (A = Sr, Ba) for La^{3+} (12);

— inserting supplementary oxygen (13);

— simultaneous formation of La^{3+} and apical $O_{(2)}$ $(LaO)^+$ vacancies (8);

(ii) a decrease of the excess negative charge of the $(BO_2)^{2-}$ equatorial planes:

— partial (B = Cu) or full (B = Ni) oxidation of B metal;

— formation of equatorial $O_{(1)}$ vacancies (14).

The overall electroneutrality of the intergrowth requires the coupling of (i) and (ii) mechanisms. This results in the well-identified crystal chemical mechanisms of formation of the cuprates (nickelates) $La_{2-x}A_xBO_{4-\delta}$, $La_2BO_{4+\delta}$ and $La_{2-\delta}BO_{4-\delta}$, where the oxygen nonstoichiometry phenomena are paired with the cationic A^{2+} substitutions or (and) the oxidation of B. This ability to oxidize the B metal, nickel, and even more copper, is a remarkable fact which affects the chemical reactivity and above all, the transport properties: the hole concentration within the equatorial Cu–O bonds is at the first rank among the parameters which govern the existence of a critical temperature of the superconducting cuprates (15).

The data on the crystal chemistry of the T-type aluminates $A^{3+}A^{2+}AlO_4$ (16, 17) confirm the validity of this analysis of the structure–bonding anisotropy and its relief. As an example, the synthesis of the substituted aluminochromite $Y_{0.9}Ca_{1.1}Cr_{0.1}Al_{0.9}O_{4-\delta}$ (18) gives evidence of simultaneous lowering of the excess positive (negative) charges of the $(YCaO_2)^+$ and $(AlO_2)^-$ slabs in the parent aluminate $YCaAlO_4$. The reported chemical mechanisms act in the same way as in the nickelates and cuprates, but their extent is less because the excess charge of the components of the intergrowth in the T-type aluminates $A^{3+}A^{2+}AlO_4$ is smaller than that in the lanthanum nickelate and cuprate.

As deduced from these data, low dimensionality in the (P)/(RS) intergrowth occurs in a cooperative system of structure–bonding anisotropic effects. Clearly, there is no pure property of any component of the intergrowth but an addition of different contributions to the overall anisotropy. Of particular importance is the achievement of a compensation of both the A–O and B–O "bonding distortions," as a result of the relief of excess anisotropy created by the initial geometrical constraint.

The information about the nature of the metal–oxygen bonding, namely the fluctuation of ionicity and covalency as obtained from electronic structure calculations, allows deeper insight into the structure–bonding anisotropy effects. The example of La_2NiO_4 (19) evidences a covalent bond order six times larger for the Ni–$O_{(1)}$ equatorial bond than for the Ni–$O_{(2)}$ apical bond. The comparison with the Ni–O bond in the nearly perfect (NiO_6) octahedra of NiO points to an increase (two times) and a decrease (three times) of the covalent bond order of the equatorial and the apical bonds, respectively. These data are rather informative as to the validity of the correlation between the bond length and the local properties of the metal–oxygen bonding: even though the overall actual charge of Ni is only slightly changed in La_2NiO_4 from NiO (80% instead of 85% of the formal value +2 (19)), the shortening (lengthening) of the equatorial (apical) Ni–O distance reveals a strong modification of the distribution of the covalency.

The (P)/(CF) Intergrowth of the T′-type Cuprates Ln_2CuO_4 (Ln = Pr–Tm)

The T'-type structure of the cuprates Ln_2CuO_4 is the 1/1 intergrowth of oxygen-deficient ABO_2 (P) slabs and AO_2 (CF) slabs, as represented by the example of Nd_2CuO_4 (20) (Fig. 2). The existence of the (P)/(CF) intergrowth is based on a simple geometrical property: the common plane of the (P) and (CF) slabs is the "A" cationic plane, i.e., the plane obtained after moving the oxygens of the "AO" plane of the (RS) slab to the typical anionic positions of the calcium fluoride structure. The mathematical condition for perfect agreement between the two slabs is

$$d_{A\text{–}O(2)}/d_{B\text{–}O(1)} = \sqrt{3}/\sqrt{2} \approx 1.225.$$

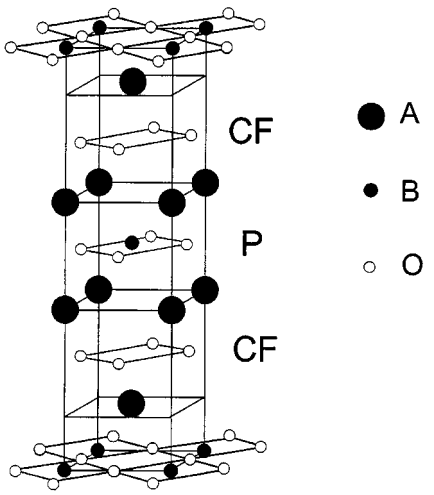

FIG. 2. (P)/(CF) intergrowth of the T'-type A_2BO_4 oxides.

The value of this ratio calculated from the ionic radii varies within the range 1.27–1.22 for the cuprates Ln_2CuO_4 (Ln = Pr–Tm). Clearly, the geometrical constraint related to the (P)/(CF) intergrowth is weak if not absent and as a consequence, the T' structure is free from any significant requirement of relief of an excess anisotropy. Therefore, the problem of the low dimensionality considered in terms of structure–bonding anisotropy can be analysed in the following way:

— In the (P)/(CF) intergrowth, the manifestation of the bidimensionality occurs in terms of a strong structure–bonding anisotropy, as visible in the lack of any apical component of the Cu–O bonding, whose dimensional extent becomes purely planar. Remarkably, such a high level of anisotropy is nearly fully consistent with the properties of the parent components of the intergrowth. For example, the typical eightfold coordination polyhedron of the (CF) structure is saved in the (P)/(CF) intergrowth.

— The absence of excess anisotropy to be relieved has a logical consequence: there is no important crystal chemical mechanism such as those reported in the (P)/(RS) intergrowth to be worked out in the (P)/(CF) intergrowth. As the main example, the oxidation of Cu(II) into Cu(III) no longer occurs and instead, the well-known property of reduction of Cu(II) into Cu(I) occurs as in the structurally unconstrained cuprates.

Examples of oxygen nonstoichiometry in the T'-type cuprates are rare. When the extent of reduction of Cu is very weak as in the substituted cuprate $Nd_{1.84}Ce_{0.16}CuO_4$ (21), the electron doping within the (CuO_2) equatorial planes is responsible for superconductivity at low temperature. The largest extent of nonstoichiometry is obtained in $Nd_2CuO_{3.5}$ (22, 23). Surprisingly, the structure of this reduced cuprate is not a modification of the T' type but belongs to the T type (23), i.e., a (P)/(RS) intergrowth where the (P) slabs are oxygen-deficient in terms of lacunar equatorial (CuO) planes and the ($Nd_2O_{2.5}$) (RS) slabs are oxygen inserted.

From this, it is possible to deduce the difference in the structure–bonding anisotropy properties of the T and T' type structures, as follows:

— The (P)/(CF) intergrowth is the best model by which to obtain the full relief of the structure–bonding constraints which originate in the formation of the (P)/(RS) intergrowth. As a matter of fact, the positions of the supplementary oxygens in the (RS) slab are precisely those which need to be occupied in a (CF) slab. Surely, a transformation of the (RS) slabs into (CF) remains fully hypothetical; nevertheless, its first step is observed in the reduced cuprate $Nd_2CuO_{3.5}$.

PECULIARITY OF THE ANISOTROPY IN THE T^*-TYPE STRUCTURE

The T^*-type structure is the 1/1 intergrowth of the T- and T'-type structures; more precisely, it is described by the following combination of slabs: (P)/(RS)/(P)/(CF) (Fig. 3a). The series of cuprates $La_{2-x-y}A_xA'_yCuO_{4-\delta}$ (A = Ba, Sr; A' = Sm–Lu, Y; $0.8 < x + y < 1$) (24, 25) present repeated examples of the T^*-type structure. The crystal chemistry of these cuprates focuses on the problem of the simultaneous stabilization of the (RS) and (CF) slabs, which requires the presence of two different A cations, a big and strongly ionic A cation and a moderately big and less ionic A' cation, which are fully ordered to ensure the existence of the (RS) and (CF) slabs, respectively. If the oxygen nonstoichiometry is not taken into account, the structural formula has to be written as follows:

$$\begin{array}{ccccccc} \text{(P)} & / & \text{(RS)} & / & \text{(P)} & / & \text{(CF)} \\ Ln_{1-x/2-y/2}A_{x/2}A'_{y/2}CuO_{2.5}/Ln_{1-x}A_xO/Ln_{1-x/2-y/2}A_{x/2}A'_{y/2}CuO_{2.5}/Ln_{1-y}A'_yO_2 & & & & & & \end{array}$$

The existence of the T^*-type structure, which was reported for the first time in the substituted neodymium cuprate $Nd_{1.32}Sr_{0.41}Ce_{0.27}CuO_{3.93}$ (26), depends on the simultaneous fulfilment of the two geometrical conditions which act separately for the T and T'-types. These conditions merge into a new one,

$$d_{Ln,A\text{–}O(2)}/d_{Ln,A'\text{–}O(3)} = 2/\sqrt{3} \approx 1.155,$$

where $d_{Ln,A\text{–}O(2)}$ is the in-plane distance in the (RS) slab and $d_{Ln,A'\text{–}O(3)}$ the out-of-plane distance in the (CF) slab (Fig. 3b). In the T^*–type structure the (RS) and the (CF) slabs have to

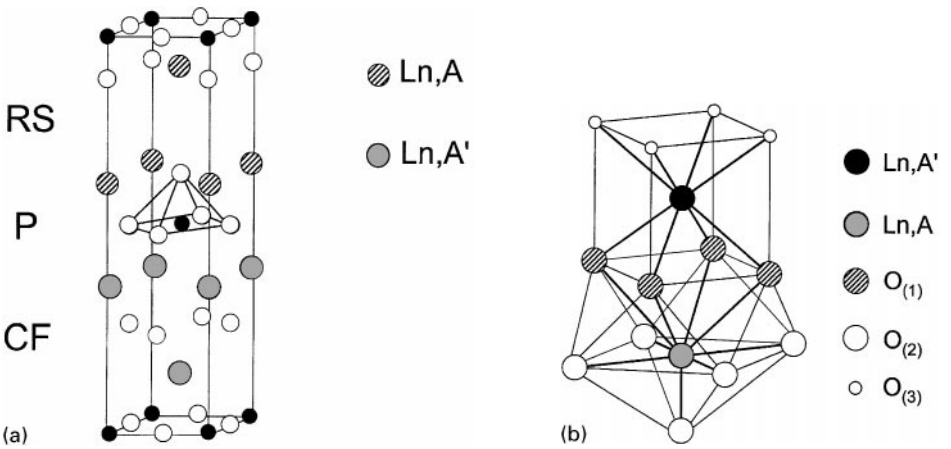

FIG. 3. (a) (P)/(RS)/(P)/(CF) intergrowth of the T^*-type A_2BO_4 oxides, (b) Connection of the eightfold and ninefold oxygen coordination polyhedra of (Ln, A') and (Ln, A).

match: such a geometrical constraint originates in the connection of the eightfold and ninefold coordination polyhedra in the (CF) and (RS) slabs, respectively (Fig. 3b).

In the series of T^*-type substituted cuprates studied up to now, i.e., the two lanthanum series $La_{2-x-y}Ba_xA'_yCuO_{4-\delta}$ (A' = Sm–Ho; Y) (24) and $La_{2-x-y}Sr_xA'_yCuO_{4-\delta}$ (A' = Sm–Lu; Y) (25) and the neodymium series $Nd_{1.2}Sr_{0.8-x}Y(Ln)_xCuO_{4-\delta}$ (Ln = Ho, Er, Yb; $0.4 < x < 0.5$; $0.11 < \delta < 0.21$) (4), recently obtained cuprates are chosen as examples where this ratio calculated from the ionic radii varies within the range 1.05–1.09. There is a weak but systematic deviation from the theoretical value, which is well taken into account by the actual structure, since the experimental value deduced from structure calculations for the neodymium series (4) is found to be close to 1.17. This means that the problem of the relief of some excess of structure–bonding anisotropy exists in the T^*-type structure but it occurs to a much smaller extent than in the T-type structure. According to the analysis for the T-type structure, the relief of the coupled underbonding–overbonding of the (AO) and (CuO_2) planes results from separate geometrical and chemical mechanisms.

Two independent geometrical mechanisms are effective, namely the shift of the apical oxygen, as in the T-type structure, and the out-of-plane shift of the equatorial oxygens, which is typical of the T^*-type structure:

— The shift of the apical oxygen toward the (Nd, Sr) metals is significantly smaller than in La_2CuO_4 (elongation close to 14% instead of 27%) and is comparable to that observed in La_2NiO_4 (16%). The Jahn–Teller effect is weakened and consequently, the apical anisotropy of the Cu–O bonding is decreased with respect to the (P)/(RS) intergrowth.

— The out-of-plane shift of the equatorial oxygens, never observed in the T'-type structure, is an original mechanism. From the structural data obtained in the case of the air-prepared neodymium cuprates $Nd_{1.2}Sr_{0.8-x}Y(Ln)_xCuO_{4-\delta}$ (Ln = Ho, Er, Yb), the value of the shift is within the range 0.19–0.30 Å. Even if it gives some relief to the overbonding in the (CuO_2) equatorial planes as in the T-type structure, it should not be confused with the buckling distortions of the (P) slabs. Such a shift also has an influence on the metal–oxygen bonding in the eightfold and ninefold coordination polyhedra of the (CF) and (RS) slabs. This is detailed further in the text.

The chemical mechanisms aim to decrease the excess charge of the different components of the intergrowth, as modeled for the T-type structure. For example, in the T^*-type structure of the cuprates $Nd_{1.2}Sr_{0.8-x}Y(Ln)_xCuO_{4-\delta}$, the components to be concerned are the $((Nd_{0.2+x}Sr_{0.8-x})_2O_2)^{(0.4+2x)+}$ (RS) slabs and the $(CuO_2)^{2-}$ equatorial planes of the (P) slabs. As in the T'-type structure, the $(Nd_{1-x}Ln_x)_2O_2$ (CF) slabs have a constant excess positive charge equal to $+2$ and consequently, have no reason to be involved in such mechanisms. The two groups of mechanisms which are deduced from the crystal chemical results are related to

(i) a decrease of the excess positive charge of the $((Nd_{0.2+x}Sr_{0.8-x})_2O_2)^{(0.4+2x)+}$ slabs

— the partial substitution of Sr^{2+} for Nd^{3+} coupled with, to some extent, both apical oxygen vacancies and supplementary inserted oxygen, already obtained in air prepared samples, in agreement with the results previously reported in the T^*-type cuprates $La_{1.2-x}Tb(Dy)_{0.8}Sr_xCuO_{4+\delta}$ and $La_{1.2}Tb_{0.8-x}Ce_xCuO_{4+\delta}$ (27);

(ii) a decrease of the excess negative charge of the $(CuO_2)^{2-}$ equatorial planes:

— some extent of equatorial oxygen vacancies in air-prepared samples and a partial oxidation of Cu(II) into Cu(III) when the samples are annealed under high p_{O_2} (1800 bars).

In the series of cuprates $Nd_{1.2}Sr_{0.8-x}Y(Ln)_xCuO_{4-\delta}$, the respective contribution of each mechanism is variable. The dependence on the crystal chemical data is rather complex: the ratio Sr/Y(*Ln*), the nature of *Ln*, and the synthesis conditions act simultaneously. Still, a basic tendency can be brought to light: due to the critical conditions of existence of the *T**-type structure, the field of action of any one of these mechanisms is restricted. Therefore, two important facts have to be pointed out

— the range of cationic substitution in the (RS) slab is small ($0.4 < x < 0.5$), as a consequence of the difference of size between Nd^{3+} and Sr^{2+}, which sets a strong constraint on the geometrical condition of existence of the *T**-type structure;

— the ability of oxidation of Cu(II) to Cu(III) is rather weak; a one-day annealing at p_{O_2} close to 20 bar and 550°C does not yield any result and a treatment at 1800 bar and 800°C is necessary to compensate for the oxygen deficiency of the air-prepared samples ($0.11 < \delta < 0.21$).

On the basis of these data, one can assume the structure–bonding anisotropy in the *T**-type structure to show a specificity with respect to (P)/(RS) and (P)/(CF) parent intergrowths. At first sight, the structure–bonding anisotropy seems to be intermediate between these two cases, as for example the fivefold pyramidal coordination of Cu. However, this picture is not valid when the actual characteristics of the anisotropic effects are considered. There is a systematic lowering of these effects, as compared to a simple addition of what is observed in the *T*- and *T*′-type structures. The low level of excess anisotropy created when matching the (RS) and (CF) slabs and consequently the rather small relief that is needed, prevent the existence of outstanding properties as for the *T*-structure. In this respect, the poor ability to oxidize Cu is of importance for the transport properties: the very weak hole concentration within the Cu–O equatorial bonds is unfavorable to the existence of a superconductive transition. Our own results confirm the absence of a critical temperature in the cuprates $Nd_{1.2}Sr_{0.8-x}Y(Ln)_xCuO_{4-\delta}$ (*Ln* = Ho, Er, Yb), even after annealing under high p_{O_2} (1800 bars). As an example, see the case of $Nd_{1.2}Sr_{0.37}Ho_{0.43}CuO_{4-\delta}$ reported in Fig. 4.

Concerning the cooperative underbonding–overbonding properties in the *T**-type structure, they cannot develop continuously through the intergrowth of the slabs as in the *T*-type structure. Their extent is limited to the path of metal–oxygen links which connects the equatorial Cu–O bonds of two nearest (P) slabs (Fig. 3a). The (CF) slabs create a barrier to further extent of these cooperative bonding effects. This sets the problem of the exact role of the structure–bonding properties in these slabs. Do they compare well with those of the (CF) slabs in the *T*′-type structure and more generally, is there some modification in the *A* metals structure–bonding properties when going from the *T* and *T*′-type structures to the *T** one?

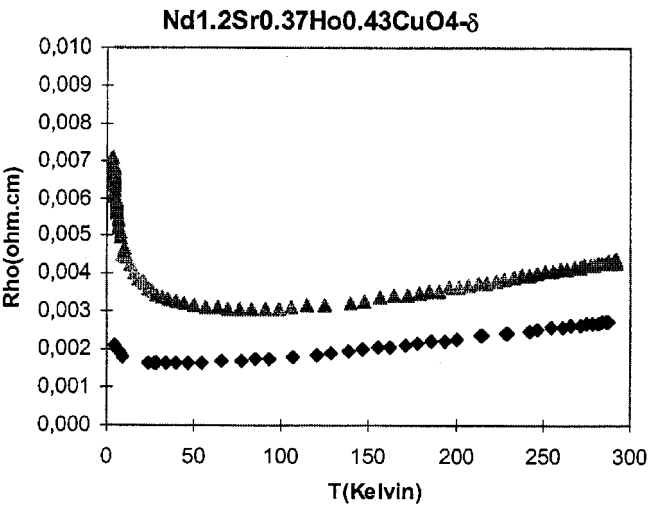

FIG. 4. Variation of the electrical resistivity versus *T* in $Nd_{1.2}Sr_{0.37}Ho_{0.43}CuO_{4-\delta}$ after annealing at high p_{O_2} (▲ 1400 and ◆ 1800 bars).

CONTRIBUTION OF THE *A*-METALS TO THE BIDIMENSIONALITY

The *A* metals present in the intergrowth structures usually have rather strong metallic properties, i.e., the actual charge of their cations is close to the formal one: for example, when *A* is a lanthanoid the charge is slightly different from +3 (approximately 90% of the formal value for La in La_2NiO_4 (19)). To picture in a good way the chemical bonding in which the *A* metals are involved, it is worth considering the role of both the attractive forces with the next oxygen neighbors and the repulsive forces between the nearest *A* cations. As regards their oxygen coordination polyhedra, the *A* metals exhibit two different cases in the (P)/(RS) and the (P)/(CF) intergrowths, respectively. Concerning the repulsive forces, an interesting geometrical characteristic has to be emphasized: there is a common *A* network in the *T*-, *T*′- and *T**-type structures.

Analysis of the Ninefold (Eightfold) Oxygen Coordination in the T- (T′)-Type Structure

The ninefold oxygen coordination polyhedron of *A* results from the "condensation" of the 12-fold and 6-fold polyhedra in the (P) and (RS) structures, respectively. It is possible to identify these two components in terms of an 8-fold (P) part and a 5-fold (RS) polyhedron (Fig. 5). The in-plane $d_{A\text{-}O(2)}$ distances play an important role, as they are common to the two components. In the *T* structure of the nickelates, cuprates, and aluminates as well, there is a systematic difference between the length of the in-plane $d_{A\text{-}O(2)}$ distances and that of the apical $d_{A\text{-}O(2)}$ one: the latter is much shorter than the former, as a consequence of the cooperative over bonding–underbonding effects. The

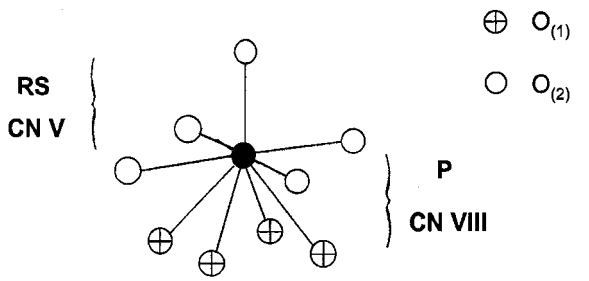

FIG. 5. Eightfold (P) and fivefold (RS) parts of the ninefold oxygen coordination of *A*.

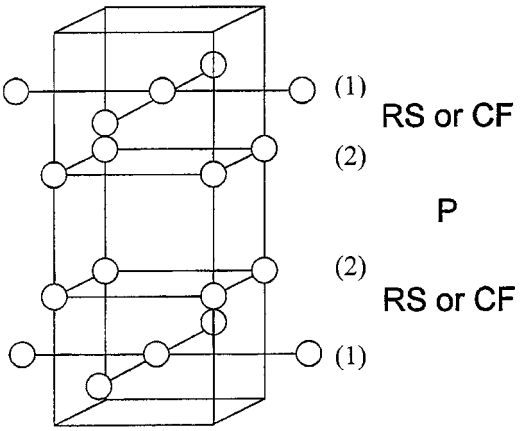

FIG. 6. *A*-network in the *T*-, *T*′-, *T**-type structures.

out-of-plane $d_{A\text{–}O(1)}$ distances remain always very close to that calculated from the ionic radii. As a result, the mean distance calculated for the (P) and (RS) parts of the 9-fold coordination is nearly unchanged (for example, no more than 0.02 Å difference in La_2NiO_4, La_2CuO_4, and LaSr(Ca)AlO_4).

The eightfold oxygen coordination polyhedron of *A* is a nonregular tetragonal prism which is the "addition" of two fourfold out-of-plane components which belong to the (P) and (CF) slabs (Fig. 5). Usually, in the *T*′-type Ln_2CuO_4 cuprates the (P) and (CF) components of the *A*–O distances are respectively longer and shorter than those calculated from the ionic radii. There is rather good compensation for this bonding anisotropy, as the mean *A*–O distance of the two components is always close to the theoretical value.

A-Network and Ninefold Cationic Coordination: A Duplicate of the Ninefold Oxygen Coordination

The common *A* network in the *T*-, *T*′- and *T**-type structures is built up from the intergrowth of identical regular 4-connected plane nets. The sequence along the *z* axis is [… (1)–(1)–(2)–(2) …], the (1) and (2) positions being face centered with respect to each other. A (1)–(1) or (2)–(2) pair of planes corresponds to a (P) slab and a (1)–(2) slab to an (RS) or a (CF) slab, as well (Fig. 6). An ideal packing of such planes requires mathematical conditions related to the interplanar spacings to be met:

$$d_{(1)\text{–}(1)} = d_{(2)\text{–}(2)} = \sqrt{2} \times d_{(1)\text{–}(2)} = 2 \times d_{B\text{–}O(1)}.$$

The fulfilment of these geometrical conditions would mean that a perfect equilibrium of the repulsive forces between the *A* cations was achieved. The analysis of the cationic coordination will point to a significant deviation from this.

The cationic coordination which exists in the *A* network, as hereabove described, is a ninefold coordination whose geometrical analysis has exactly the same basis as the ninefold oxygen coordination of *A* in the *T*-type structure (Fig. 7). More precisely, it includes an eightfold (RS) part and a fivefold (P) part (Fig. 7). Clearly, this ninefold cationic coordination is a duplicate of the ninefold oxygen coordination where the contributions of the (P) and (RS) parts are exchanged. The nine shortest *A*–*A* distances consist in two groups of four distances, the in-plane and the out-of-plane group, plus the apical distance which can be considered as the thickness of a (P) slab. The values calculated for these distances in La_2NiO_4, La_2CuO_4, $LaCaAlO_4$, and Nd_2CuO_4 are the following:

A′–*A* distances (Å)	La_2NiO_4	La_2CuO_4	$LaCaAlO_4$	Nd_2CuO_4
Out of plane (×4)	4.12	3.98	3.74	3.72
In plane (×4)	3.87	3.81	3.72	3.94
Apical	3.25	3.66	3.50	3.62
(RS) part	3.99	3.89	3.73	3.83
				Δ[P–CF]
(P) part	3.75	3.78	3.68	3.88
Δ[P–RS]	0.24	0.11	0.05	0.05
				((CF) part)

The distortion of the ninefold cationic coordination is systematic, but its extent varies significantly. In the series of the three *T*-type oxides, the difference between the values of

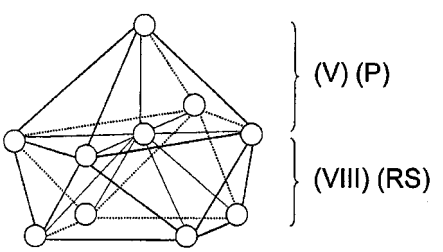

FIG. 7. Fivefold (P) and eightfold (RS) parts of the ninefold cationic coordination of *A*.

the La–La(Ca) distances (La^{3+} and Ca^{2+} have nearly the same ionic radius) in the two parts of the coordination, i.e., Δ[P–RS], decreases from the nickelate to the cuprate and further to the aluminate where it is small. In the same way, a rather weak distortion is found for the T'-type structure of Nd_2CuO_4. As the most striking feature, the apical distance, as in the ninefold oxygen coordination, is the shortest. In terms of structure–bonding anisotropy, these data are meaningful:

— the repulsive forces between the A cations occur first within the (P) slab.

In this respect, La_2NiO_4 is at the first rank: the value 3.25 Å for a La^{3+}–La^{3+} distance is much smaller than in La_2O_3 (3.94 Å (28)). One can find here another reason to understand the ability to get coupled (La–O) vacancies in the oxides $La_{2-x}NiO_{4-x}$ (8) since it results in a decrease of the La^{3+}–La^{3+} repulsive forces. Compared to La_2NiO_4, La_2CuO_4 exhibits a large increase of this apical distance: this is not surprising, as the (P) slab is much more elongated due to the Jahn–Teller effect of Cu^{2+}. $LaCaAlO_4$ (28) presents an intermediate example between La_2NiO_4 and La_2CuO_4: in so far as a half of the A cations are Ca^{2+}, there is a decrease of the repulsive forces and a stabilization of the (RS) slab, resulting in an overall weakening of the structure–bonding anisotropy. As to the T'-type structure of Nd_2CuO_4, the value 3.62 Å for a Nd^{3+}–Nd^{3+} distance is not as small (3.83 Å in Nd_2O_3 (28)), this being consistent with the absence of Cu–O apical bonding.

Cooperative Properties of the Oxygen and Cationic Coordination of the A-Metals: A Supplementary Contribution to the Bidimensionality of the T-type Structure

The T-type structure has a unique characteristic: the geometrical analysis of the oxygen and cationic coordination of its A metals is common. More precisely, the theoretical model is the same and, that is informative for the anisotropy of structure bonding, the distortion is similar. Figure 8 gives evidence of this. Owing to the existence of apical shifts of both the oxygen anions and the A cations, a series of cooperative variations of the structure–bonding properties occur in agreement with a pairing of an overbonding (underbonding) of the A–O links and an "overrepulsing" ("underrepulsing") of the A–A repulsive interactions, as deduced from Fig. 8. These cooperative properties concern three groups of A–O links and A–A interactions which are paired in the following ways:

— the overbonding of the apical A–O bond with the overrepulsing of the A–A interaction (Fig. 9a), as the strongest effect;

— the underbonding of the four in plane A–O bonds with the underrepulsing of the four out of plane A–A interactions (Fig. 9b), as a weaker effect;

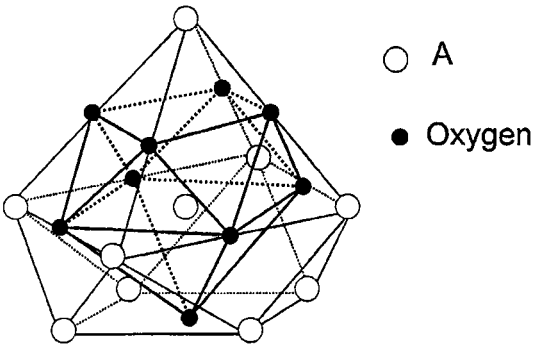

FIG. 8. Ninefold cationic and oxygen coordination polyhedra of A.

— the simultaneous lack of variation of the bonding and the repulsive properties of the four out-of-plane A–O bonds and the four-in-plane A–A interactions, respectively (Fig. 9c).

These cooperative properties occur systematically in the T-type structure and their contribution to the two-dimensionality cannot be neglected. Of particular importance is the combined role of the apical attractive A–O forces and repulsive A–A one which are created by the A–metals in the intergrowth of a (P) and a (RS) slab. If one assumes that the apical A–A overrepulsing overcomes the apical A–O overbonding, there will be, as a result, a weakening of the apical link in the intergrowth. This must be considered as a supplementary contribution to the apical B–O underbonding in the octahedra of the (P) slab: the addition of these effects will create the overall two dimensionality of the T-type structure. As deduced from the data above reported, this supplementary contribution is the largest in La_2NiO_4.

For the T'-type structure, none of these cooperative structure–bonding properties can be obtained. The A–A repulsive forces remain to some extent whose contribution to the 2D is likely a weak one in comparison with that of the absence of apical Cu–O bonding.

Specific Structure–Bonding Properties of the A(A′)-Metals in the T-Type Structure*

In the T*-type structure the two kinds of oxygen coordination of the $A(A')$ metals, i.e., the ninefold and the eightfold coordinations occur simultaneously. The basis of the geometrical analysis reported for these coordinations when they exist separately in the T- and T'-type structures, is always valid. However, the precise data related to their distortion are modified in the following way:

— there is a common tendency to obtain a more regular distribution of the A–O (A'–O) distances in the ninefold and eightfold coordination, respectively.

The origin of this specific property of the T*-type structure has to be found in a cooperative effect between the

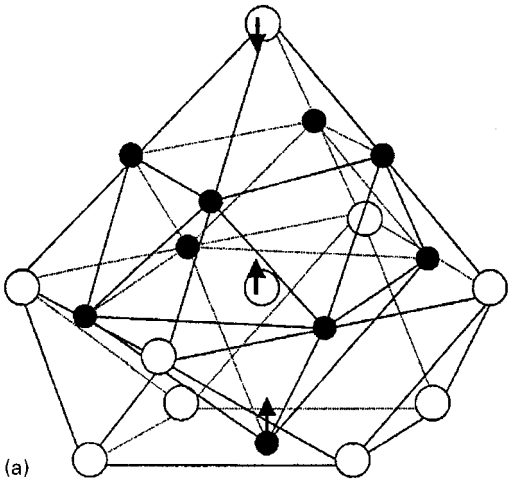

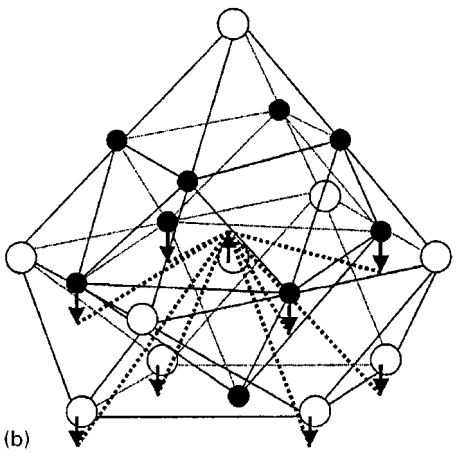

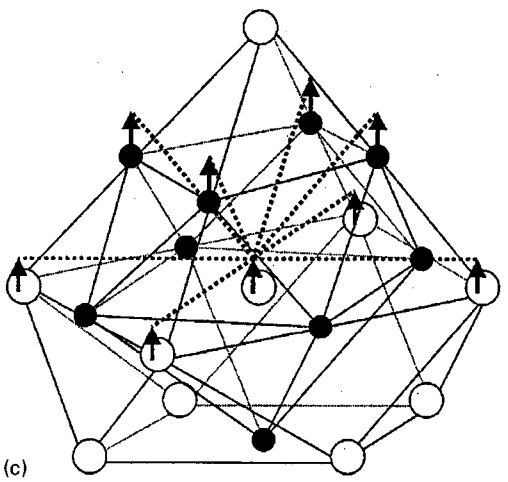

FIG. 9. Cooperative variations of the structure–bonding properties created by the apical shifts of the oxygens anions (●) and *A*-cations (○). (a) Cooperative overbonding of the apical *A*–O bond and overrepulsing of the *A*–*A* interaction. (b) Cooperative underbonding of the in plane *A*–O bonds and underrepulsing of the out of plane *A*–*A* interactions. (c) Simultaneous lack of variation of the bonding and the repulsive properties of the out of plane *A*–O bonds and in plane *A*–*A* interactions.

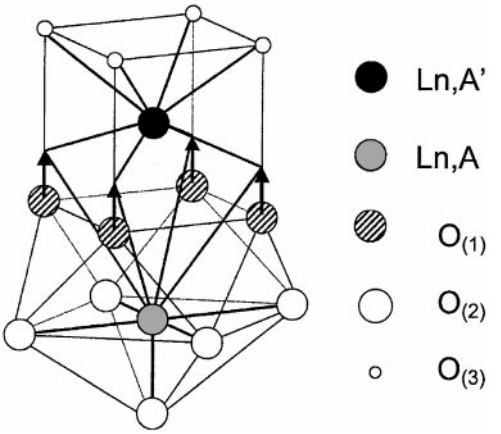

FIG. 10. Apical shift of the equatorial $O_{(1)}$ oxygens in the *T**-type structure.

ninefold and eightfold coordination polyhedra which is created by the apical shift of the equatorial $O_{(1)}$ oxygens of the square face shared by these two polyhedra (Fig. 10). As a consequence, there is a simultaneous lengthening and shortening of the out-of-plane $d_{A\text{-}O(1)}$ and $d_{A'\text{-}O(1)}$ distances, respectively. This means that the deviation between the out-of-plane $d_{A\text{-}O(1)}$ and in-plane $d_{A\text{-}O(2)}$ distances (ninefold coordination) and equally the deviation between the out-of-plane $d_{A'\text{-}O(1)}$ and $d_{A'\text{-}O(3)}$ distances (eightfold coordination) is significantly lowered. As an example, in the latter case the large deviation close to 0.35 Å in the series of *T*′-type Ln_2CuO_4 cuprates (29) decreases to a value nearly constant and equal to 0.08 Å in the *T**-type cuprates $Nd_{1.2}Sr_{0.8-x}Y(Ln)_xCuO_{4-\delta}$ (Ln = Ho, Er, Yb) herein reported. In the same way, these *T** cuprates have a very small deviation between the in-plane and out-of-plane *A*–O distances (ninefold coordination), 0.03 Å more for the out-of-plane distances, instead of 0.15 Å more for the in-plane distances in La_2CuO_4 (7). Finally, only the apical $A\text{–}O_{(2)}$ distance which is typical of the (P)/(RS) intergrowth remains rather small, 0.30 Å shorter than the other *A*–O distances in ninefold coordination. This fact allows one to think of the existence of cooperative properties of the ninefold oxygen and cationic coordinations similar to that occurring in the *T* type structure.

The *A*(*A*′)-network in the *T**-type structure has the same theoretical description as in the *T*- and *T*′-types, but its actual geometrical characteristics are somewhat modified due to the existence of an order of the *A*- and *A*′ metals whose crystallographic positions in the cell are independent. Consequently, there are two sets of ninefold cationic coordinations, $A\text{–}(A_8A')$ and $A'\text{–}(A'_8A)$ (Fig. 11). The values of the distances, as obtained for the cuprate $Nd_{1.2}Sr_{0.4}Er_{0.4}CuO_{4-\delta}$, are

— one apical *A*–*A*′ distance, 3.54 Å;
— four in-plane *A*–*A* (*A*′–*A*′) distances, 3.83 Å;

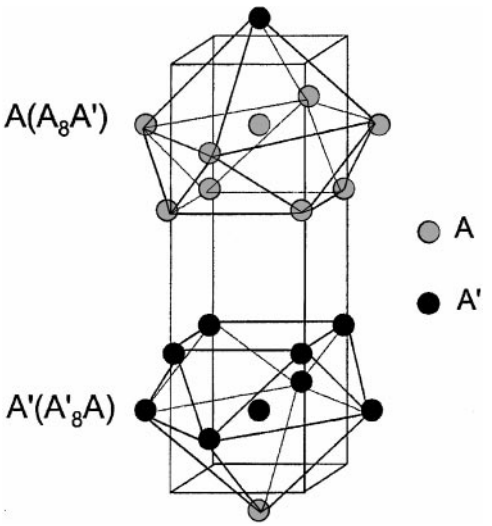

FIG. 11. Two sets of ninefold cationic coordination polyhedra in the T^*-type structure.

— two sets of four out-of-plane distances, A–A 3.87 Å and A'–A' 3.80 Å.

The two polyhedra differ very slightly from each other: there is a small deviation between the four out-of-plane distances. Otherwise, the common important feature concerns the short apical A–A' distance. Interestingly, this distance is lowered with respect to the same distance in both the T- and T'-type cuprates La_2CuO_4 and Nd_2CuO_4, 3.66 and 3.62 Å, respectively. As the value 3.54 Å is an average of four distances, Nd^{3+}–Nd^{3+}, Nd^{3+}–Er^{3+}, Sr^{2+}–Nd^{3+}, and Sr^{2+}–Er^{3+}, the precise level of the repulsive forces is difficult to appreciate. Still, undoubtly there is a significant apical A–A' overrepulsing whose coupling with the apical A–O overbonding will weaken the apical link of the (P)/(RS) part of the T^*-type structure. Such a contribution to the bidimensionality can be assumed reasonably to exceed which is observed in La_2CuO_4. In contrast, in the case of the apical Cu–O underbonding which, in the T^*-type structure, is not so effective as in the T-type one, the apical A'–A–O structure–bonding anisotropy is of importance in the occurrence of the bidimensionality of the T^*-type structure.

CONCLUSION

Intergrowth oxides, as built up from the connection of slabs of different 3D compact structures by means of common crystallographic planes, are the best candidates to characterize the occurrence of the bidimensionality. The structure–bonding anisotropy is the very first mark of the bidimensionality: it originates in the geometrical constraint which results from the matching of a (P) slab with a (RS) or (CF) one. The analysis of the anisotropy reveals the systematic occurrence of a series of cooperative structure– bonding properties whose extent is variable depending on the proper intergrowth to be considered, namely the T, T', or T^*-types. In any case, the common trend of this anisotropy consists in an overbonding in the (BO_2) equatorial planes coupled with an overall underbonding of the apical link. In terms of local properties of the chemical bonding, it seems very likely that the distribution of the covalency, above all in the B–O bonds, is changed at the expense of the apical component which is decreased as the equatorial one is strongly increases. Still, the balance of the ionicity and the covalency of the metal–oxygen bonds is not significantly modified, this being consistent with the usually high stability of these intergrowths which compares well with that of the parent structures.

Interestingly, the weakening of the apical link is obtained on the basis of cooperative effects which involve attractive metal–oxygen forces and repulsive A–metal interactions. In this respect, the underbonding of the apical B–O component (T-type structure) or even more its absence (T'-type structure) play a main role. As a supplementary contribution, the apical A–A repulsive interactions are able to balance the apical A–O overbonding. This is of particular importance in the T-type structure due to the identity of the geometrical characteristics of the oxygen and cationic ninefold coordination of the A metals. When the apical B–O underbonding is large as in La_2CuO_4, the contribution of the apical A–A repulsive interactions is not very important; conversely when it is reduced as in La_2NiO_4, the apical La^{3+}–La^{3+} repulsion ($d_{La^{3+}\text{-}La^{3+}} = 3.25$ Å) has to be taken into account to understand the existence of a high structure–bonding anisotropy.

In the manifestation of the bidimensionality, particular emphasis has to be layed on the excess structure–bonding anisotropy correlated with the excess of electrostatic charge in the components of the intergrowth. This correlation occurs systematically in the (P)/(RS) intergrowth of the T-type oxides, but it is unknown in the (P)/(CF) intergrowth of the T'-type oxides since the excess anisotropy is absent. The larger is the excess anisotropy, the larger equally is the excess charge in both the cationic and anionic components. The relief of the excess anisotropy is achieved by crystal chemical mechanisms whose driving force is the simultaneous decrease of the excess positive charge in the (A_2O_2) (RS) slabs and the excess negative charge in the (BO_2) equatorial planes. The pairing of the oxygen nonstoichiometry phenomena with the cationic A substitutions or (and) the oxidation of B is exemplified by oxides where the B metal is not necessarily a transition metal (Ni, Cu) but a p element such as Al. When the extent of excess anisotropy is not so large, as in the double intergrowth of the T^*-type oxides, the working of such crystal chemical mechanisms is restricted, i.e., the cationic A substitutions and the oxidation of B are limited. In this respect, the T^*-type oxides exhibit a supplementary limitation of these mechanisms owing to

a cooperative property of the ninefold and eightfold oxygen coordination of the $A(A')$ metals in the (RS) and (CF) slabs, respectively, which makes the distribution of the A–O bonding forces more regular and further induces a decrease of the overall structure–bonding anisotropy.

As a way to conceive new oxide materials whose dimensionality is intermediate between the three-dimensionality of compact structures and the two-dimensionality of layer structures, the creation of a controlled excess structure–bonding anisotropy seems to be a fruitful idea. In so far as it is possible to correlate geometrical and bonding constraints in an intergrowth of slabs, namely to get cooperative effects of both the structural distortions and the charge distribution, rich properties are expected. Of major interest is the ability to a high chemical reactivity which involves various components of the oxide solid state chemistry: the most remarkable one is the large extent of oxygen nonstoichiometry, as frequently connected to the existence of outstanding physical properties.

ACKNOWLEDGMENTS

We are indebted to Dr. J. Karpinski, Solid State Physics Laboratory, E. T. H. Zürich, for the annealings of the T^* cuprates at high p_{O_2}.

REFERENCES

1. J. Rouxel, L'Actualité Chimique, Société Française *de Chimie* **3,** 5 (1998).
2. J. Rouxel, *NATO ASI Ser. B* **354,** 1 (1996).
3. J. Rouxel and E. Evain, *Eur. J. Solid State Inorg. Chem.* **31,** 683 (1994).
4. G. Caruntu, Doctorate thesis, Orléans University (1998).
5. R. D. Shannon, *Acta Crystrallogr. Sect. A* **32,** 751 (1976).
6. J. M. Longo and P. M. Raccah, *J. Solid State Chem.* **6,** 526 (1973).
7. J. Choisnet, J. M. Bassat, H. Pillière, P. Odier, and M. Leblanc, *Solid State Commun.* **66,** 1245 (1988).
8. I. Zvereva, L. Zueva, and J. Choisnet, *J. Mater. Sci.* **30,** 3598 (1995).
9. I. D. Brown, *Acta Crystallogr. Sect. B* **48,** 553 (1992).
10. J. D. Jorgensen, B. Dabrowski, S. Pei, D. R. Richards, and D. G. Hinks, *Phys. Rev. B* **40,** 2187 (1989).
11. J. Rodriguez-Carjaval, M. T. Fernandez-Diaz, and J. L. Martinez, *J. Phys. Condens. Matter* **3,** 3215 (1991).
12. Z. Kakol, J. Spalek, and J. M. Honig, *J. Solid State Chem.* **79,** 288 (1989).
13. A. Demourgues, F. Weill, B. Darriet, A. Wattiaux, J. C. Grenier, P. Gravereau, and M. Pouchard, *J. Solid State Chem.* **106,** 317 (1993).
14. N. Nguyen, J. Choisnet, M. Hervieu, and B. Raveau, *J. Solid State Chem.* **39,** 120 (1981).
15. M. Muroi, *Phys. C* **219,** 129 (1994).
16. Y. P. Oudalov, A. Daoudi, J. C. Joubert, G. Le Flem, and P. Hagenmuller, *Bull. Soc. Chim. Fr.* **10,** 3408 (1970).
17. F. Archaimbault, J. Choisnet, and I. Zvereva, *Mater. Chem. Phys.* **34,** 300 (1993).
18. I. Zvereva, L. Zueva, F. Archaimbault, M. Crespin, J. Choisnet, and J. Lecomte, *Mat. Chem. Phys.* **48,** 103 (1997).
19. J. Choisnet, R. A. Evarestov. I. I. Tupitsyn, and V. Veryazov, *J. Phys. Chem. Solids* **57,** 1839 (1996).
20. H. Müller-Buschbaum, *Angew. Chem. Int. Edeng.* **16,** 674 (1977).
21. Y. Tokura, H. Tagaki, and S. Ushida, *Nature* **337,** 345 (1989).
22. F. C. Chou, J. H. Cho, L. L. Miller, and D. C. Johnston, *Phys. Rev. B* **42,** 6172 (1990).
23. J. Choisnet, P. Mouron, M. Crespin, P. A. Van Aken, and W. Müller, *J. Mater. Chem.* **4,** 895 (1994).
24. E. M. Kopnin, E. V. Antipov, and L. M. Kovba, *Superconductivity* **5,** 1793 (1992).
25. E. M. Kopnin, R. V. Shpanchenko. E. V. Antipov, and L. M. Kovba, *Superconductivity* **5,** 1787 (1992).
26. H. Sawa *et al.*, *Nature* **337,** 347 (1989).
27. A. Lappas and K. Prassides, *J. Solid State Chem.* **115,** 332 (1995).
28. E. F. Westrum, Jr., "Progress in the Science and Technology of the Rare Earths" (L. Eyring, Ed.), Vol. 1, p. 310, Pergamon Press, New York, 1964.
29. Yr. Smirnof, I. Zvereva, and J. Choisnet, *J. Solid State Chem.* **134,** 132 (1997).
30. Ph. Galez and G. Collin, *J. Phys. France* **51,** 579 (1990).